







Ti₃C₂/ε-Ga₂O₃ Schottky Self-Powered Solar-Blind Photodetector With Robust Responsivity

Zu-Yong Yan , Shan Li , Zeng Liu , Wen-Jie Liu, Fen Qiao, Pei-Gang Li, Xiao Tang, Xiao-Hang Li ,
Jian-Ying Yue, Yu-Feng Guo , *Member, IEEE*, and Wei-Hua Tang 

Abstract—As a 2D material, MXene has emerged as an excellent electrode material for optoelectronic devices due to its high conductivity and hydrophilic surface. Here, the Ti₃C₂-based MXene was employed to construct the Ti₃C₂/ε-Ga₂O₃ Schottky junction photodetector. The fabricated device demonstrated a self-powered operation manner with an extremely low dark current (0.07 pA), an outstanding light on/off switch ratio (2.5×10^6), a remarkable photo-response speed (43 ms/145 ms), a responsivity (R) of 15.5 mA/W, an external quantum efficiency (EQE) of 7.5% and a detectivity (D*) of 2.15×10^{11} Jones. Such excellent photodetection performance that is comparable or even higher than those of Ga₂O₃ Schottky photodetectors previously reported are originated from the excellent conductivity of MXene, good crystallization of ε-Ga₂O₃, and their well-matched energy level. Additionally, our Schottky junction device is capable of sensing solar-blind UV region and exhibits excellent stability in the air environment. The perfect combination of 2D MXene and wide-bandgap ε-Ga₂O₃ proposes a novel route for the self-powered Schottky devices.

Index Terms—MXene, ε-Ga₂O₃, self-powered photodetector, Schottky junction.

Manuscript received May 27, 2021; accepted October 29, 2021. Date of publication November 4, 2021; date of current version December 8, 2021. This work was supported in part by the National Natural Science Foundation of China under Grant 61774019, in part by the Fund of State Key Laboratory of Information Photonics and Optical Communications (Beijing University of Posts and Telecommunications), and in part by the Fundamental Research Funds for the Central Universities, China. (Corresponding authors: Fen Qiao; Pei-Gang Li; Wei-Hua Tang.)

Zu-Yong Yan, Shan Li, Pei-Gang Li, and Jian-Ying Yue are with the Laboratory of Information Functional Materials and Devices, School of Science and State Key Laboratory of Information Photonics and Optical Communications, Beijing University of Posts and Telecommunications, Beijing 100876, China (e-mail: zyyan@bupt.edu.cn; lishan1989@bupt.edu.cn; pgl@bupt.edu.cn; yue-jianying@bupt.edu.cn).

Zeng Liu, Yu-Feng Guo, and Wei-Hua Tang are with the College of Electronic and Optical Engineering and College of Microelectronics, National and Local Joint Engineering Laboratory for RF Integration and Micro-Packaging Technologies, Nanjing University of Posts and Telecommunications, Nanjing, Jiangsu 210023, China (e-mail: zengliu@njupt.edu.cn; yfguo@njupt.edu.cn; whtang@njupt.edu.cn).

Wen-Jie Liu and Fen Qiao are with the School of Energy and Power Engineering, Jiangsu University, Zhenjiang, Jiangsu 212013, China (e-mail: 953303317@qq.com; fqiao@ujs.edu.cn).

Xiao Tang and Xiao-Hang Li are with the Advanced Semiconductor Laboratory, King Abdullah University of Science and Technology, Thuwal 23955-6900, Saudi Arabia (e-mail: xiao.tang@kaust.edu.sa; xiaohang.li@kaust.edu.sa).

This article has supplementary material provided by the authors and color versions of one or more figures available at <https://doi.org/10.1109/JSTQE.2021.3124824>.

Digital Object Identifier 10.1109/JSTQE.2021.3124824

I. INTRODUCTION

THE emergence of 2D materials and their heterostructures with fascinating electronic and optical properties provided an additional opportunity for building optoelectronic and electronic devices [1], [2]. A new branch of 2D materials, including transition metal carbides, carbonitrides, and nitrides, namely MXenes, was initially discovered by Barsoum *et al.* in 2011 [3]. The excellent performances such as high conductivity and hydrophilic surface indicate that MXenes can be good candidates for electronics and optoelectronics materials [4], [5]. The 2D MXenes based 2D-2D and 2D-3D van der Waals (vdW) heterostructures, are of unique ability to interact with other materials without being restricted by lattice matching, hence have recently attracted intense interest. However, the further applications of 2D-2D vdW heterostructures in large-scale and high-integrated devices is severely suffered from the small size and the complicated transfer process [6]. Compared to the 2D-2D vdW heterostructures, the 2D-3D vdW heterostructures that combine the advantages of 2D materials with the desired functions of the developed semiconductors are ideal in promising applications. In particular, MXenes based 2D-3D vdW heterostructures such as MXene/silicon [7], MXene/perovskite [8], and MXene/GaAs [9], etc. have been marginally designed for photodetectors (PDs) [10]. Inspired by all of these, reasonable selection of the semiconductors and serious-minded design of the interface are of the great significance toward exploring excellent 2D heterostructures for advanced performance PDs [11].

As an ultra-wide bandgap semiconductor, Ga₂O₃ sparks wide interest for the building of solar-blind PDs because it holds several advantages over other materials, such as instant solar-blind UV absorption with a wide bandgap (~ 4.9 eV), excellent thermal and chemical stability [12]–[20]. Ga₂O₃ has five phases of α , β , γ , δ and ϵ . Among these polymorphs, the β -phase is investigated most extensively for optoelectronics. In contrast, other metastable phases have been studied less, but they also have unique application characteristics in device applications [21]. The ϵ phase Ga₂O₃ has hexagonal and orthorhombic crystal structure. Therefore, the ε-Ga₂O₃, as a kind of Ga₂O₃ isomer, is increasing of great interest [22]. For instance, Chao and Mishra revealed that a two-dimensional electron gas is formed at the ε-Ga₂O₃/CaCO₃ interface with a charge density of 10^{14} cm⁻², which is two orders of magnitude higher than

that formed at the $(\text{Al}_x\text{Ga}_{1-x})_2\text{O}_3/\beta\text{-Ga}_2\text{O}_3$ interface [23]. In addition, $\varepsilon\text{-Ga}_2\text{O}_3$ UV PDs have been investigated by lots of research groups, including ours, and these PDs have significant UV detection capabilities [24]–[27].

Here, based on the MXene/ $\varepsilon\text{-Ga}_2\text{O}_3$ Schottky junction heterostructure, a self-powered solar-blind UV PD with high responsivity (15.5 mA W^{-1}), ultralow dark current (0.07 pA), and high light on/off ratio (2.5×10^6) under zero biasing voltage at 254 nm was devised. Moreover, to get more understanding into the inherent mechanism of the PD, the dependence of response time on the light intensity and running modes has been investigated in detail. Also, the device without packaging already exhibits excellent stability after exposure under ambient temperature for 45 days, showing the great potential of using MXene/ $\varepsilon\text{-Ga}_2\text{O}_3$ Schottky junction as a promising low energy-cost self-powered solar-blind UV detectors or solar-blind UV photocells.

II. EXPERIMENTS

A. $\varepsilon\text{-Ga}_2\text{O}_3$ Film Growth

An $\varepsilon\text{-Ga}_2\text{O}_3$ layer was epitaxially grown on a (0001) sapphire substrate, carrying via a customized MOCVD growth system with a reaction chamber. Triethylgallium (TEGa) and O_2 were taken as gallium and oxygen precursor, respectively. TEGa and Oxygen gas were transported by the carrier gas (Ar) into the growth chamber. The growth process was carried out under the conditions of 25 Torr pressure and 470°C temperature, and maintain 60 mins.

B. Synthesis of Ti_3C_2

Ti_3AlC_2 (MAX phase) powder (1 g) was dispersed in a mixture solution of 9 M HCl (20 mL) and LiF (1 g), followed by stirring at room temperature for 24 h to etch Al atom. The acidic suspension was washed with deionized water via centrifugation (3500 rpm for 3 min) several times, until $\text{pH} \geq 6$. The resulting suspension was redispersed in deionized water and then centrifuged at 3500 rpm for 1 h. The suspension containing single-layer 2D Ti_3C_2 nanoflakes was obtained and further used for later drop-casting.

C. Device Preparation

After the epitaxial deposition of the $\varepsilon\text{-Ga}_2\text{O}_3$ film, the colloidal solution of prepared Ti_3C_2 was drop casted on the $\varepsilon\text{-Ga}_2\text{O}_3$ surface. After drying at 40°C for 10 h, the silver and indium electrodes were fabricated on Ti_3C_2 and $\varepsilon\text{-Ga}_2\text{O}_3$ thin films, respectively (Fig. 2a). The distance between the In electrode and Ti_3C_2 is $308 \mu\text{m}$.

D. Characterization and Measurement

The crystal structure and micromorphology features of the as-prepared samples were obtained using X-ray diffraction (XRD, D8 Advance, Bruker), scanning electron microscopy (SEM, S4800, Hitachi) and transmission electron microscopy (TEM,

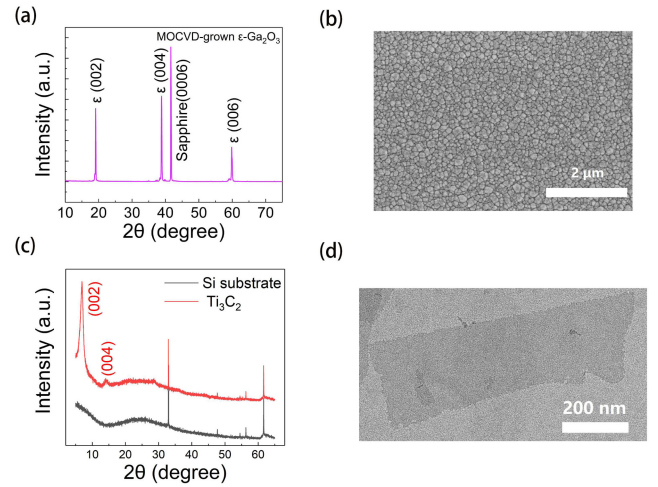


Fig. 1. (a) XRD θ - 2θ scan of the $\varepsilon\text{-Ga}_2\text{O}_3$ film; (b) SEM image of the $\varepsilon\text{-Ga}_2\text{O}_3$ film; (c) XRD pattern of the Ti_3C_2 film; (d) TEM image of the Ti_3C_2 .

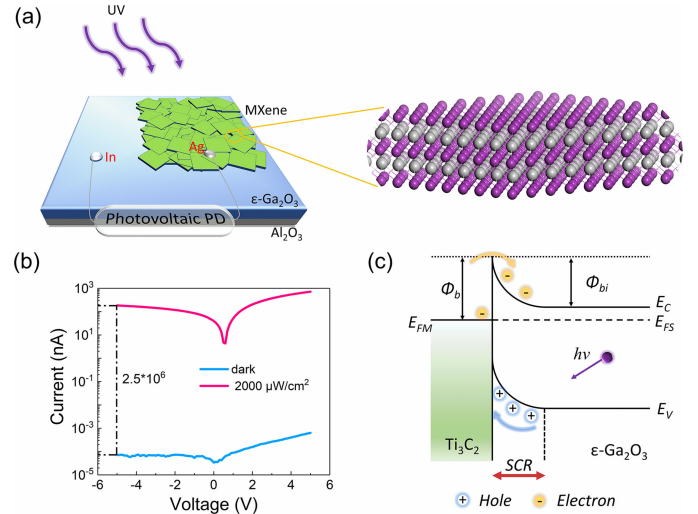


Fig. 2. (a) The schematic diagram of the $\text{Ti}_3\text{C}_2/\varepsilon\text{-Ga}_2\text{O}_3$ Schottky photo-voltaic PD. The inset is the crystal structure of Ti_3C_2 , where the purple and gray balls correspond to Ti and C atoms, respectively. (b) I-V characteristic of the Schottky PD with and without 254 nm UV light ($2000 \mu\text{W}/\text{cm}^2$) in logarithmic scale. (c) Electron energy level diagrams of the Schottky PD with no applied voltage.

Tecnai G2 F30, FEI), respectively. The optical absorption spectrum measurement of the film was tested by UV-vis spectroscopy (UV-1800PC, China). The spectroscopic photoresponse of the device was measured using a monochromator combined. The photoelectric performance was recorded using a UV lamp as a light source, and a semiconductor characterization system (Keithley 4200), respectively.

III. RESULTS AND DISCUSSION

The XRD pattern shows diffraction peaks at 19.11° , 38.83° and 59.83° (Fig. 1a), which are assigned to the (002), (004) and (006) planes of the orthorhombic crystal structure of the $\varepsilon\text{-Ga}_2\text{O}_3$ film, respectively. The value of FWHM for (002) plan is 0.145. The result indicates a (002)-single preferred orientation

of the $\varepsilon\text{-Ga}_2\text{O}_3$ film. In addition, the FWHM of $\varepsilon\text{-Ga}_2\text{O}_3$ (002) plan is 2242 arcsec obtained from the rocking curve (Fig. S1). The SEM image is also acquired on the surface of the sample as shown in Fig. 1b, indicating a fine-grained morphology of the thin film. d. The thickness of $\varepsilon\text{-Ga}_2\text{O}_3$ film is 350 nm measured from the cross-section SEM, as shown in Fig. S2.

The UV-vis absorption spectrum of the prepared $\varepsilon\text{-Ga}_2\text{O}_3$ film is shown in Fig. S3, from which the obtained band gap (E_g) of the $\varepsilon\text{-Ga}_2\text{O}_3$ film is 4.92 eV by extrapolating the line of the Tauc diagram to the x-axis of photon energy (inset of Fig. S3).

For investigations of phase information of Ti_3C_2 , Ti_3C_2 was drop casted on Si substrate. The corresponding XRD spectra of Ti_3C_2 MXene sheets are shown in Fig. 1c, where the peaks of (002) and (004) planes are found at $2\theta = 6.9^\circ$ and 14.0° , respectively. Besides, the morphology of the Ti_3C_2 sheets was characterized by using TEM as shown in Fig. 1d.

The schematic diagram of the $\text{Ti}_3\text{C}_2/\varepsilon\text{-Ga}_2\text{O}_3$ Schottky junction PD is presented in Fig. 2a. The inset of Fig. 2a shows the schematic of Ti_3C_2 , where the purple and gray balls correspond to Ti and C atoms, respectively.

Fig. 2b depicts the I-V behavior of the Schottky PD, the dark current of the Schottky PD is ultralow (≈ 0.07 pA at -5 V), which is significantly lower compared to those of the Schottky junction Ga_2O_3 -based PDs in previous reports[51]. First, such a low dark current can be attributed to a relatively low concentration of defects in the high crystalline quality $\varepsilon\text{-Ga}_2\text{O}_3$ film. Second, the formation of a “space charge region” (SCR) between the surface of Ti_3C_2 MXene and $\varepsilon\text{-Ga}_2\text{O}_3$ might lead to a surface barrier, which could also reduce the dark current. The value of the photo-dark current ratio (I_p/I_d) is 2.5×10^6 , confirming that the device has a high signal-to-noise ratio and high-quality photosensitive switching characteristic.

The working mechanism of the $\text{Ti}_3\text{C}_2/\varepsilon\text{-Ga}_2\text{O}_3$ Schottky PD could be explicated from the energy band configuration, as illustrated in Fig. 2c, where Φ_b is the Schottky barrier height, E_{FM} is the Fermi-level of the Ti_3C_2 MXene, E_{FS} is the Fermi-level of the $\varepsilon\text{-Ga}_2\text{O}_3$, E_C is the conduction band, E_V is the valance band, and Φ_{bi} is the built-in potential. The work function (W_M) of the Ti_3C_2 is 4.6 eV and the electron affinity(χ) of Ga_2O_3 is 4 eV, respectively, so the value of Φ_b is 0.6 eV [28], [29]. The $\varepsilon\text{-Ga}_2\text{O}_3$ and Ti_3C_2 generate a Schottky junction and form an SCR in the $\varepsilon\text{-Ga}_2\text{O}_3$ side. The Schottky junction is dominated by a majority of carrier transport. The direction of the built-in electric field is pointing from $\varepsilon\text{-Ga}_2\text{O}_3$ to Ti_3C_2 . Under light illumination, the photon-generated carriers in or near the SCR are separated and conducted by the internal driving force (built-in electric field). In this configuration, the holes are transported to Ti_3C_2 , while the electrons are collected by the In electrode through $\varepsilon\text{-Ga}_2\text{O}_3$, forming the photocurrent.

Another important characteristic of the PD is the dependence of photocurrent with light intensity. The current-voltage characteristics of the device at 254 nm illumination of different intensities are shown in Figs. S4 and 3a (high resolution). The results indicate that the photocurrent of the Schottky junction PD has a strong dependence on the light intensities. The photocurrent increases with the illumination intensity, since the density of

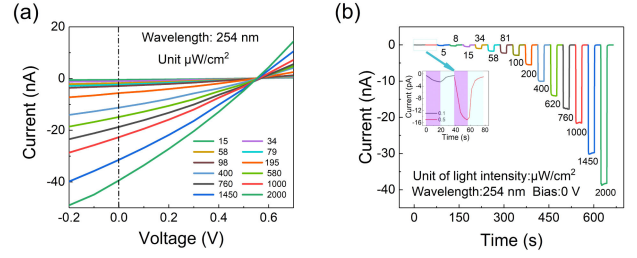


Fig. 3. (a) I-V behaviors of Schottky PD at different illumination intensities with 0 V. (b) Photoresponse of $\text{Ti}_3\text{C}_2/\varepsilon\text{-Ga}_2\text{O}_3$ Schottky PD under different UV illumination intensities at zero bias.

the photoexcited carrier is proportional to the luminous flux absorbed.

Fig. 3b shows the photoresponse switching behavior of the Schottky junction PD under repeated light on/off cycles at 0 V under illumination with intensities varying from $0.1 \mu\text{W}/\text{cm}^2$ to $2000 \mu\text{W}/\text{cm}^2$. Even under the ultralow light intensity of $0.1 \mu\text{W}/\text{cm}^2$, the photo-to-dark current switch ratio of the photo signal is 5, indicating an excellent photoresponse capability under the weak signals.

Fig. S5 shows the incident optical power-dependent output electrical signal. The dependence is given by $I_{ph} = kP^\theta$, where, I_{ph} is the photocurrent, k is constant for a particular wavelength, P is the input optical power, the θ is the empirical value related to the complex process of trapping, and recombination within the device, which was estimated as 0.818 by fitting. This linear variation of the photocurrent suggests that the Schottky junction PD has obvious intensity-dependent features and can be fabricated for accurate solar-blind UV detection.

The response time is the capacity of a PD to respond to a changing incident light signal. Generally, it is defined as “ON” and “OFF” or “recovery” times. The devices operated in photovoltaic and photoconductive modes are also expected to have different transient light switching characteristics. We compared the performance of photo-switching characteristics of the $\text{Ti}_3\text{C}_2/\varepsilon\text{-Ga}_2\text{O}_3$ Schottky photovoltaic PD with metal-semiconductor-metal (MSM) pristine In/ $\varepsilon\text{-Ga}_2\text{O}_3$ /In conductive PD (Fig. 4a). The distance of In electrodes of conductive device is about $280 \mu\text{m}$. Fig. 4b shows the transient photocurrent response at 254 nm for the two types of PDs with a bias voltage of 0 V and -0.1 V, respectively. In order to accurately compare the response speed of the two devices at the same photocurrent (10 nA), the Schottky device and the conductive device were tested under $400 \mu\text{W}/\text{cm}^2$ and $600 \mu\text{W}/\text{cm}^2$ UV illumination, respectively. In the absence of light irradiation, the $\text{Ti}_3\text{C}_2/\varepsilon\text{-Ga}_2\text{O}_3$ Schottky PD shows an ultralow dark current, only at the pA level. Even without an external bias voltage, when the light is “turned on”, the photocurrent reached \sim nA; while the signal is “turned off”, the current rapidly returns to the initial value. The results clearly show that Schottky PD has obvious and stable transient photo-response characteristics. The rise/decay times are obtained by fitting the curves using the formula (1a) and

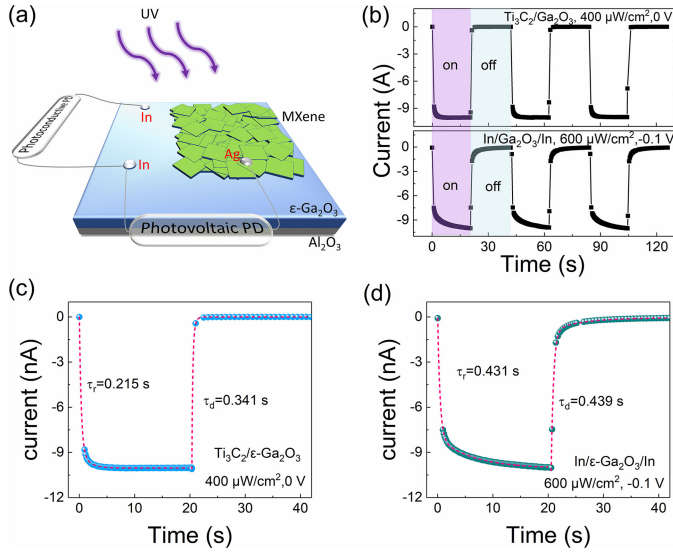


Fig. 4. (a) The schematic diagram of the Ti₃C₂/ε-Ga₂O₃ Schottky photovoltaic PD and In/ε-Ga₂O₃/In conductive PD. (b) Photoresponse of Ti₃C₂/ε-Ga₂O₃ PD and In/ε-Ga₂O₃/In PD. The response speed of (c) The Ti₃C₂/ε-Ga₂O₃ photovoltaic detector at 0 V and (d) the In/ε-Ga₂O₃/In conductive detector at -0.1 V.

(1b)

$$I(t) = I_0 \exp\left(-\frac{t}{\tau_r}\right) - I_0 \quad (1a)$$

$$I(t) = I_0 - I_0 \exp\left(-\frac{t}{\tau_d}\right) \quad (1b)$$

where I_0 is the value of current when illumination is in turned on/turned off states, and τ_r and τ_d are the rise time and decay time. The values of the rise and decay times are fitted to be 215 and 341 ms for Schottky PD (Fig. 4c), 431 and 439 ms for conductive PD (Fig. 4d), respectively. Compared with the conductive PD without Ti₃C₂ electrode, the response speed of the Schottky PD with Ti₃C₂ nanosheets electrode is improved and faster, which shows that using Ti₃C₂ as Schottky contact causes an obvious improvement of the response speed of the device because of the construction of the built-in potential.

In addition to operating under the photovoltaic mode, Schottky PD could work in the photoconductive mode, i.e., under applied voltage. To further analyses the response times of the Schottky PD under both the forward voltage and reverse voltage, the transient response of the Schottky photovoltaic PD under 15 μW/cm² illumination at different voltages is displayed in Fig. 5a. The photocurrent at the reverse bias is less than those at the forward bias because of rectifying effect, but response speed at the reverse voltage is faster than those at the forward voltage. Obviously, as shown in Figs. 5b and 5c, under 15 μW/cm², the rise/decay times of 0.79 s/0.109 s at -4 V are much shorter than those of 2.518 s/0.429 s at 4 V. A possible mechanism is proposed to explain above results. Compared with the condition of working under forward bias, more photogenerated electrons and holes are swept and then transferred toward the corresponding

electrodes, due to the widening of the SCR and higher field in the SCR under the reverse bias (Fig. 5e and 5f). Thus, it exhibits a faster response at the reverse voltage.

We further analyze the variation of the response time with applied biases. As shown in Fig. 5d, the τ_r increases with applied bias, while τ_d decreases with applied bias. (This situation is similar to that whether the Schottky device operates at forward bias or reverse bias). Such a dependence where rise times increase with bias might be caused by the persistent photo-conductivity (PPC). At higher biasing voltages, the application of a high electric field makes these photogenerated carriers be released from defect centers (such as oxygen vacancies), resulting in a high photoconductance gain, but at the cost of a slower photodetection speed [30]. The decrease in the decay time with the applied bias is due to the higher applied bias and the faster drift velocity [31].

Figs. 6a and 6b show response time of the Ti₃C₂/ε-Ga₂O₃ Schottky photovoltaic device and In/ε-Ga₂O₃/In conductive device at different illumination power densities with a bias voltage of 0 V and -0.1 V, respectively. The response speed has a similar tendency with power density, in which the τ_r and τ_d decrease with the illumination intensities, a phenomenon attributed to the trap filling. The photocurrent transients are influenced by the filling of traps, which are most pronounced when the injection level is raised with increasing photon flux. The most remarkable effect of the higher light density is the shortening of the rise and decay time. This general observation is due to the filling of deep trap states which lose their influence in the early stage of the photocurrent transient. This means that trap filling is more easily excited at stronger optical intensities, and hence improves the transport behavior (response speed) [32], [33]. Apparently, as the optical powers increase, the response time for Ti₃C₂/ε-Ga₂O₃ Schottky PD decreases faster than that of In/ε-Ga₂O₃/In conductive PD. The built-in electric field at the Ti₃C₂/ε-Ga₂O₃ interface is essential to improve separation and transportation of the photogenerated electrons and holes, and therefore promoting a more rapid response speed. The results were consistent with those shown in Fig. 4(b, c, d).

Responsivity (R), external quantum efficiency (EQE), and special detectivity (D*) are critical FOMs (Figure of Merit) for PDs and are related to each other, which is provided in Fig. 6c.

The responsivity of PD can be written as.

$$R = \frac{I_p - I_d}{P \times S} \quad (2)$$

Here I_p , I_d , P , and S represent the photocurrent, dark current, light intensity, light signal exposed area. Fig. 6c shows the R vs light intensities plot, which decreases with increasing light intensities. The high responsivity (15.5 mA/W) at lower illumination intensity (0.1 μW/cm²) indicates outstanding performance in the sensing of low optical power. The responsivity of our PD is higher than other Schottky junction Ga₂O₃ PDs [8]–[12], because of the high crystallization of ε-Ga₂O₃ and excellent conductive of Ti₃C₂.

The EQE, which is used to describe the ratio number of electrons excited to the number of incident photons, is described

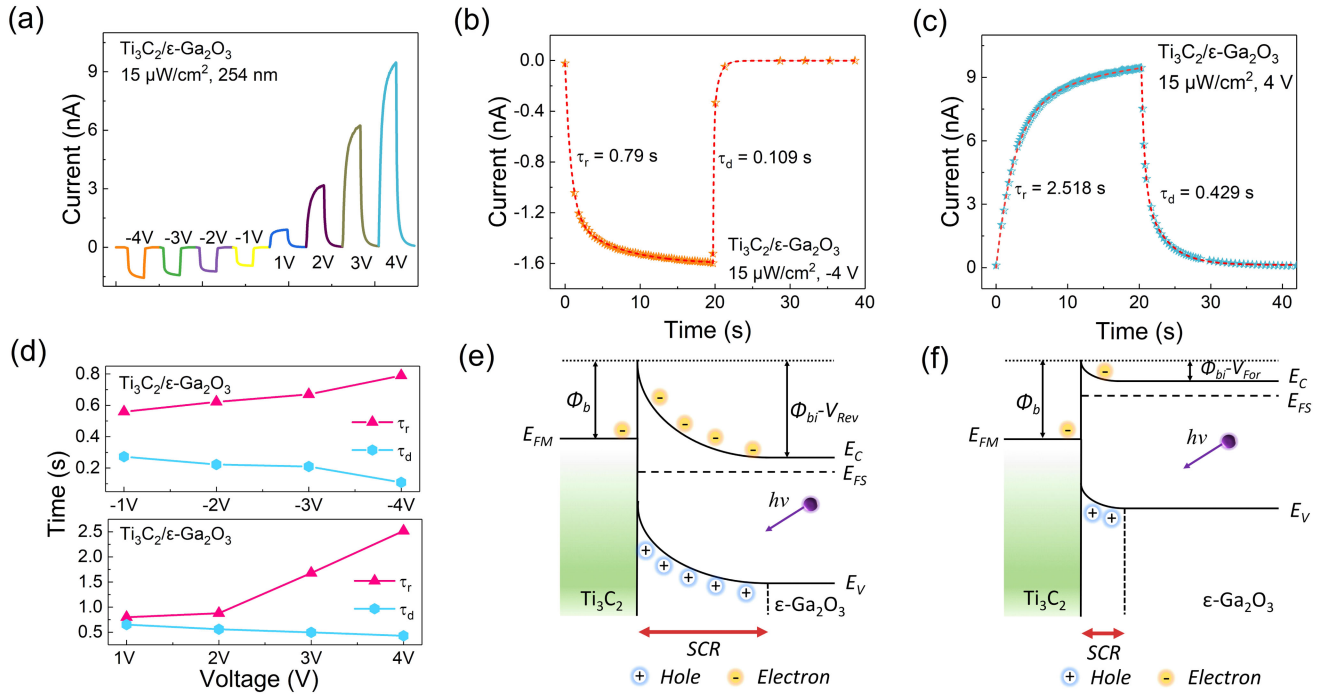


Fig. 5. (a) The photoresponse performance of the Schottky photovoltaic PD at different bias. The response times of the $\text{Ti}_3\text{C}_2/\varepsilon\text{-Ga}_2\text{O}_3$ Schottky junction PD at (b) -4 V and (c) 4 V. (d) The variation of response speed with applied bias. Electron energy level diagrams of the device: (e) with applied reverse bias (f) with applied forward bias.

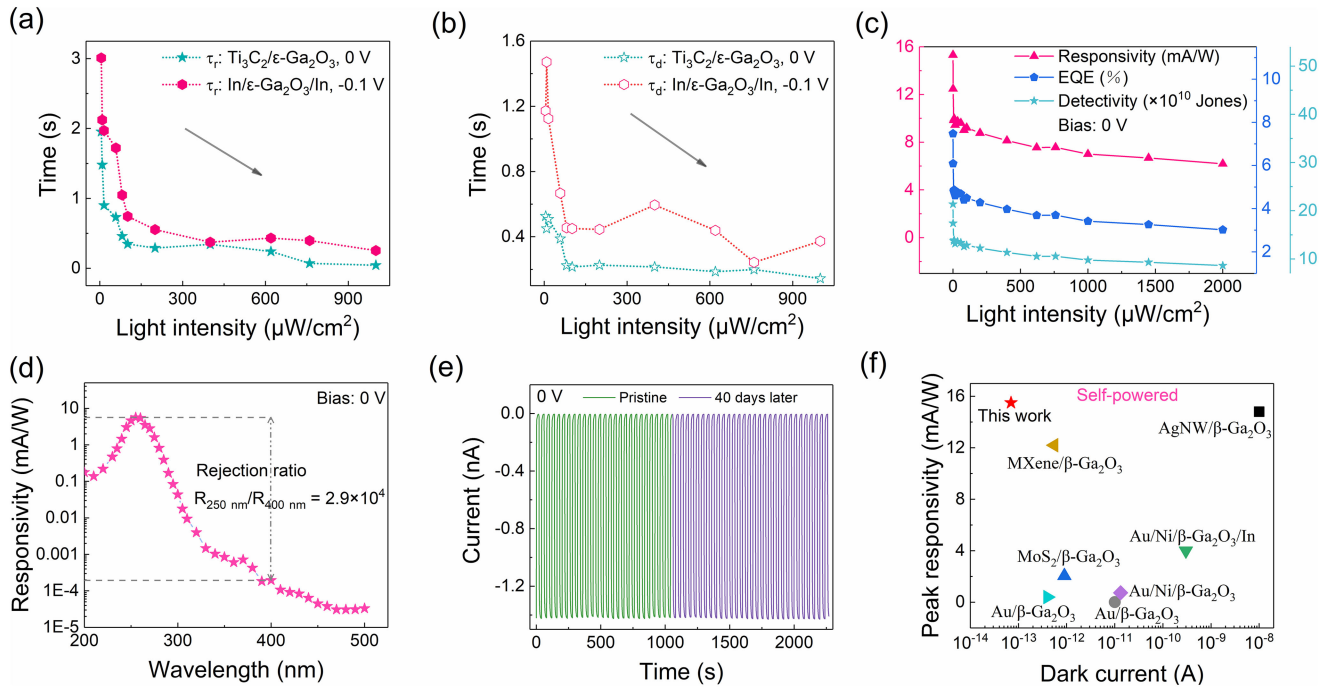


Fig. 6. (a) The rise and (b) decay times of the Schottky PD and conductive PD with different light intensities at 0 V and -0.1 V, respectively. (c) The R, EQE, and D^* of Schottky PD as a function of 254 nm illumination intensity at 0 V. (d) Wavelength-dependent responsivity of the Schottky PD at 0 V bias. (e) Time-dependent response of the photovoltaic PD measured at as-prepared and after 40 days at 0 V. (f) Responsivity and dark current of our device and other previously reported Ga_2O_3 Schottky self-powered PDs.

TABLE I
THE DEVICE PARAMETERS COMPARISON OF PDS BASED ON Ga₂O₃ SCHOTTKY JUNCTION

Materials	Self-powered	Dark Current	PDCR (Light Intensity)	Responsivity (mA/W)	D*	EQE (%)	Rise/Decay time	Rejection Ratio	Reference
Mxenes/ ϵ -Ga ₂ O ₃	yes	0.07 pA (-5 V)	1.2×10^6 (2 mW/cm ²)	15.5	2.15×10^{11}	7.5	43/145 ms	2.9×10^4 (R ₂₅₅ /R ₄₀₀)	This work
Au/ β -Ga ₂ O ₃	yes	10 pA (-30 V)	$>1 \times 10^3$ (2 mW/cm ²)	0.01			-1/64 μ s	$\frac{38}{(R_{258}/R_{400})}$	[34]
MoS ₂ / β -Ga ₂ O ₃	yes	0.9 pA	670 (20 μ W/cm ²)	2.05	1.21×10^{11}			1.6×10^3 (R ₂₅₄ /R ₄₀₀)	[35]
Au/Ni/ β -Ga ₂ O ₃ /In	yes	300 pA (5V)	10^2	4		3	90/170 ms	10^3	[36]
Au/Ni/ β -Ga ₂ O ₃	yes	13.2 pA (-10 V)	2.83×10^5 (220 μ W/cm ²)	0.73	3.35×10^{10}	0.36		4.8×10^3 (R ₂₅₀ /R ₄₀₀)	[17]
Mxenes/ β -Ga ₂ O ₃	yes	0.55 pA	1.6×10^4 (115.1 μ W/cm ²)	12.2	6.1×10^{12}	6.2	8/131 μ s	2.4×10^2 (R ₂₅₀ /R ₄₀₀)	[37]
Au/ β -Ga ₂ O ₃	yes	0.4 pA (-20V)	10^5 (1 mW/cm ²)	0.4	1.8×10^{12}		290/50 ms		[38]
Graphene/ β -Ga ₂ O ₃ /Graphene	no	0.1 pA (10 V)	1.18×10^4	29800 (10 V)	1.45×10^{12} (10 V)			9.4×10^3 (R ₂₅₄ /R ₃₆₅)	[39]
AgNW/ β -Ga ₂ O ₃	yes	10 pA	1.2×10^5 (216 μ W/cm ²)	14.8	5.1×10^{12}	7.2	20 ms/24 ms	2.6×10^3 (R ₂₅₄ /R ₃₆₅)	[40]
Au/Ni/ β -Ga ₂ O ₃	yes			9780	3.29×10^{14}		5 μ s	10^4 (R ₂₁₂ /R ₃₅₀)	[41]

by:

$$EQE = R \frac{hc}{\lambda q} \quad (3)$$

Here h , c , λ , and q represent Planck's constant, the speed of light, the wavelength, and the quantity of charge. The variation in EQE at different light illumination intensities for Schottky PD is shown in Fig. 6c and the EQE has a maximum value of 7.5 at the minimum illumination intensity.

D^* , which is utilized to describe the smallest detectable signal, is derived as follows.

$$D^* = \frac{\sqrt{S} \cdot R}{\sqrt{2qI_d}} \quad (4)$$

The incident light illumination intensity-dependent D^* at 0 V are shown in Fig. 6c. We note that D^* decreases with the incident illumination intensity and reaches a maximum value of up to 2.15×10^{11} Jones at the minimum light density, indicating the device has the ability to detect the weak solar-blind UV light. The aforementioned response characterizations indicate an excellent performance of Ti₃C₂/ ϵ -Ga₂O₃ PD in terms of high sensitivity to weak-light detection. The value of R, EQE, and D^* decrease with increasing light intensity, which can be attributed to self-heating.

To further investigate the working wavelength range of the Schottky PD, the responsivity is measured in the range from 200 to 500 nm at zero bias (Fig. 6d). The responsivity of the device with a maximum value of ~ 5.6 mA/W at 255 nm, is negligible to visible light, which closely matches the UV-*vis* absorption spectra in Fig. S3. For example, the UV-*vis* rejection ratio (R_{255nm}/R_{400nm}) is found to be 2.9×10^4 , confirming that Ti₃C₂/ ϵ -Ga₂O₃ Schottky PD owns high wavelength selectivity with low background noise and could be a good solar-blind UV-sensitive PD.

The stability of PD is considered, as a significant challenge for their practical application and commercialization, therefore it was investigated by testing the performance upon the exposure to air environment for 40 days under multi-cycle 254 nm UV illuminating at zero bias (Fig. 6e). The unchanged photocurrent indicates the excellent stability of the PD.

As shown in Fig. 6f, the Ti₃C₂/ ϵ -Ga₂O₃ Schottky PD concomitantly shows high responsivity and low dark current, compared to the other self-powered Schottky junction Ga₂O₃ PDs. For a more comprehensive comparison, Table I lists the critical parameters of Schottky PDs based on the Ga₂O₃, including our work and other previously reported studies. Compared with other Ga₂O₃ Schottky PDs, our device shows higher responsivity, EQE, rejection ratio, lower dark current, moderate detectivity, and response speed. The superior performance indicates that our Ti₃C₂/ ϵ -Ga₂O₃ Schottky PD is a greatly promising candidate for the fabrication of high responsivity and low noise PDs.

IV. CONCLUSION

In summary, a self-powered Schottky junction solar-blind PD was constructed by combing the drop-casted Ti₃C₂ layer and the MOCVD deposited ϵ -Ga₂O₃ layer. Such UV PD exhibits high responsivity of 15.5 mA/W, EQE of 7.5%, rejection ratio of 2.9×10^4 , ultra-low dark current of 0.07 pA, and high I_p/I_d of 2.5×10^6 at zero bias, overall showing superior performances compared to the previously reported Ga₂O₃ based Schottky self-powered PDs. The high performance of Schottky PD may well be attributed to the high crystal quality of ϵ -Ga₂O₃, excellent conductivity of Ti₃C₂, and built-in field at the ϵ -Ga₂O₃/Ti₃C₂ interface. With the introduction of the internal photovoltaic effect, the rise time and decay time are greatly decreased compared with photoconductive ϵ -Ga₂O₃-based photodetectors. Meanwhile, the device exhibits outstanding stability and wavelength selectivity as well. This work highlights a feasible strategy to develop a photoelectronic device with high performance in a self-powered mode.

REFERENCES

- [1] S. J. Liang, B. Cheng, X. Cui, and F. Miao, "Van der Waals heterostructures for high-performance device applications: Challenges and opportunities," *Adv Mater*, vol. 32, no. 27, 2020, Art. no. e1903800.
- [2] Z. Wu, W. Jie, Z. Yang, and J. Hao, "Hybrid heterostructures and devices based on two-dimensional layers and wide bandgap materials," *Mater. Today Nano*, vol. 12, 2020, Art. no. 100092.
- [3] M. Naguib *et al.*, "Two-dimensional nanocrystals produced by exfoliation of Ti₃AlC₂," *Adv. Mater.*, vol. 23, no. 37, pp. 4248–4253, 2011.

- [4] K. Hantanasirisakul and Y. Gogotsi, "Electronic and optical properties of 2D transition metal carbides and nitrides (MXenes)," *Adv. Mater.*, vol. 30, no. 52, 2018, Art. no. e1804779.
- [5] Y. H. Yao *et al.*, "All-optical modulator using MXene inkjet-printed microring resonator," *IEEE J. Sel. Topics Quantum Electron.*, vol. 26, no. 5, pp. 1–6, Sep./Oct. 2020.
- [6] Z. Lu *et al.*, "Ultrahigh speed and broadband few-layer MoTe_2/Si 2D–3D heterojunction-based photodiodes fabricated by pulsed laser deposition," *Adv. Funct. Mater.*, vol. 30, no. 9, 2020, Art. no. 1907951.
- [7] Z. Kang *et al.*, "MXene-silicon van der Waals heterostructures for high-speed self-driven photodetectors," *Adv. Electron. Mater.*, vol. 3, no. 9, 2017, Art. no. 1700165.
- [8] W. Deng *et al.*, "All-sprayed-processable, large-area, and flexible perovskite/MXene-based photodetector arrays for photocommunication," *Adv. Opt. Mater.*, vol. 7, no. 6, 2019, Art. no. 1801521.
- [9] K. Montazeri *et al.*, "Beyond gold: Spin-coated Ti_2C_3 -based MXene photodetectors," *Adv. Mater.*, vol. 31, no. 43, 2019, Art. no. e1903271.
- [10] H. Xu, A. B. Ren, J. Wu, and Z. M. Wang, "Recent advances in 2D MXenes for photodetection," *Adv. Funct. Mater.*, vol. 30, no. 24, 2020, Art. no. 2000907.
- [11] T. Yang *et al.*, "Ultrahigh-performance optoelectronics demonstrated in ultrathin perovskite-based vertical semiconductor heterostructures," *ACS Nano*, vol. 13, no. 7, pp. 7996–8003, 2019.
- [12] X. H. Chen, F. F. Ren, S. L. Gu, and J. D. Ye, "Review of gallium-oxide-based solar-blind ultraviolet photodetectors," *Photon. Res.*, vol. 7, no. 4, pp. 381–415, 2019.
- [13] A. S. Pratiyush, S. Krishnamoorthy, R. Muralidharan, S. Rajan, and D. N. Nath, "Advances in Ga_2O_3 solar-blind UV photodetectors," in *Gallium Oxide*, Amsterdam, Netherlands: Elsevier, 2019, pp. 369–399.
- [14] S. J. Pearton *et al.*, "A review of Ga_2O_3 materials, processing, and devices," *Appl. Phys. Rev.*, vol. 5, no. 1, 2018, Art. no. 011301.
- [15] Y. Qin *et al.*, "Enhancement-mode $\beta\text{-Ga}_2\text{O}_3$ metal-oxide-semiconductor field-effect solar-blind phototransistor with ultrahigh detectivity and photo-to-dark current ratio," *IEEE Electron Device Lett.*, vol. 40, no. 5, pp. 742–745, May 2019.
- [16] S. Li *et al.*, "Ultrasensitive, superhigh signal-to-noise ratio, self-powered solar-blind photodetector based on $\text{n-Ga}_2\text{O}_3/\text{p-CuSCN}$ core-shell microwire heterojunction," *ACS Appl. Mater. Interfaces*, vol. 11, no. 38, pp. 35105–35114, 2019.
- [17] Z. Liu *et al.*, "A high-performance ultraviolet solar-blind photodetector based on a $\beta\text{-Ga}_2\text{O}_3$ Schottky photodiode," *J. Mater. Chem. C*, vol. 7, no. 44, pp. 13920–13929, 2019.
- [18] S. Li *et al.*, "Broadband ultraviolet self-powered photodetector constructed on exfoliated $\beta\text{-Ga}_2\text{O}_3/\text{CuI}$ core-shell microwire heterojunction with superior reliability," *J. Phys. Chem. Lett.*, vol. 12, no. 1, pp. 447–453, 2021.
- [19] Z. Yan *et al.*, "High sensitivity and fast response self-powered solar-blind ultraviolet photodetector with a $\beta\text{-Ga}_2\text{O}_3/\text{spiro-MeOTAD p-n}$ heterojunction," *J. Mater. Chem. C*, vol. 8, no. 13, pp. 4502–4509, 2020.
- [20] M. K. Yadav, A. Mondal, S. Shringi, S. K. Sharma, and A. Bag, "Performance enhancement of $\beta\text{-Ga}_2\text{O}_3$ on Si (100) based Schottky barrier diodes using REDuced SURface field," *Semicond. Sci. Technol.*, vol. 35, no. 8, 2020, Art. no. 085009.
- [21] X. H. Hou *et al.*, "Review of polymorphous Ga_2O_3 materials and their solar-blind photodetector applications," *J. Phys. D: Appl. Phys.*, vol. 54, no. 4, 2021, Art. no. 043001.
- [22] F. Mezzadri *et al.*, "Crystal structure and ferroelectric properties of $\varepsilon\text{-Ga}_2\text{O}_3$ films grown on (0001)-sapphire," *Inorganic Chem.*, vol. 55, no. 22, pp. 12079–12084, 2016.
- [23] S. B. Cho and R. Mishra, "Epitaxial engineering of polar $\varepsilon\text{-Ga}_2\text{O}_3$ for tunable two-dimensional electron gas at the heterointerface," *Appl. Phys. Lett.*, vol. 112, no. 16, 2018, Art. no. 162101.
- [24] Z. Liu *et al.*, "Fabrication of $\varepsilon\text{-Ga}_2\text{O}_3$ solar-blind photodetector with symmetric interdigital Schottky contacts responding to low intensity light signal," *J. Phys. D: Appl. Phys.*, vol. 53, no. 29, 2020, Art. no. 295109.
- [25] Y. Cai *et al.*, "Tin-assisted growth of $\varepsilon\text{-Ga}_2\text{O}_3$ film and the fabrication of photodetectors on sapphire substrate by PLD," *Opt. Mater. Exp.*, vol. 8, no. 11, pp. 3506–3517, 2018.
- [26] Y. Qin *et al.*, "High-performance metal-organic chemical vapor deposition grown $\varepsilon\text{-Ga}_2\text{O}_3$ solar-blind photodetector with asymmetric Schottky electrodes," *IEEE Electron Device Lett.*, vol. 40, no. 9, pp. 1475–1478, Sep. 2019.
- [27] S. Li *et al.*, "Oxygen vacancies modulating the photodetector performances in $\varepsilon\text{-Ga}_2\text{O}_3$ thin films," *J. Mater. Chem. C*, vol. 9, no. 16, pp. 5437–5444, 2021.
- [28] Z. Wang, H. Kim, and H. N. Alshareef, "Oxide thin-film electronics using all-MXene electrical contacts," *Adv. Mater.*, vol. 30, no. 15, 2018, Art. no. e1706656.
- [29] M. Mohamed *et al.*, "Schottky barrier height of Au on the transparent semiconducting oxide $\beta\text{-Ga}_2\text{O}_3$," *Appl. Phys. Lett.*, vol. 101, no. 13, 2012, Art. no. 132106.
- [30] Y. F. Zhang *et al.*, "Transition of photoconductive and photovoltaic operation modes in amorphous Ga_2O_3 -based solar-blind detectors tuned by oxygen vacancies," *Chin. Phys. B*, vol. 28, no. 2, 2019, Art. no. 028501.
- [31] Z. Liu *et al.*, "Comparison of optoelectrical characteristics between Schottky and Ohmic contacts to $\beta\text{-Ga}_2\text{O}_3$ thin film," *J. Phys. D: Appl. Phys.*, vol. 53, no. 8, 2020, Art. no. 085105.
- [32] X. Li *et al.*, "High-performance photoelectrochemical-type self-powered UV photodetector using epitaxial $\text{TiO}_2/\text{SnO}_2$ branched heterojunction nanostructure," *Small*, vol. 9, no. 11, pp. 2005–2011, 2013.
- [33] J. van de Lagemaat and A. J. Frank, "Nonthermalized electron transport in dye-sensitized nanocrystalline TiO_2 films: transient photocurrent and random-walk modeling studies," *J. Phys. Chem. B*, vol. 105, no. 45, pp. 11194–11205, 2001.
- [34] X. Chen *et al.*, "Self-powered solar-blind photodetector with fast response based on $\text{Au}/\beta\text{-Ga}_2\text{O}_3$ nanowires array film Schottky junction," *ACS Appl. Mater. Interfaces*, vol. 8, no. 6, pp. 4185–4191, 2016.
- [35] R. Zhuo *et al.*, "A self-powered solar-blind photodetector based on a $\text{MoS}_2/\beta\text{-Ga}_2\text{O}_3$ heterojunction," *J. Mater. Chem. C*, vol. 6, no. 41, pp. 10982–10986, 2018.
- [36] A. S. Pratiyush *et al.*, "MBE-grown $\beta\text{-Ga}_2\text{O}_3$ -based Schottky UV-C photodetectors with rectification ratio $\sim 10^7$," *IEEE Photon. Technol. Lett.*, vol. 30, no. 23, pp. 2025–2028, Dec. 2018.
- [37] Y. Chen *et al.*, "Solar-blind photodetectors based on MXenes- $\beta\text{-Ga}_2\text{O}_3$ Schottky junctions," *J. Phys. D: Appl. Phys.*, vol. 53, no. 48, 2020, Art. no. 484001.
- [38] Y. Zhi *et al.*, "Self-powered $\beta\text{-Ga}_2\text{O}_3$ solar-blind photodetector based on the planar $\text{Au}/\text{Ga}_2\text{O}_3$ Schottky junction," *ECS J. Solid State Sci. Technol.*, vol. 9, no. 6, 2020, Art. no. 065011.
- [39] S. Oh, C.-K. Kim, and J. Kim, "High responsivity $\beta\text{-Ga}_2\text{O}_3$ metal-semiconductor-metal solar-blind photodetectors with ultraviolet transparent graphene electrodes," *ACS Photon.*, vol. 5, no. 3, pp. 1123–1128, 2017.
- [40] P. Tan *et al.*, "Balancing the transmittance and carrier-collection ability of Ag nanowire networks for high-performance self-powered Ga_2O_3 Schottky photodiode," *Adv. Opt. Mater.*, vol. 9, no. 15, 2021, Art. no. 2100173.
- [41] Y. Xu *et al.*, "Fast speed Ga_2O_3 solar-blind Schottky photodiodes with large sensitive area," *IEEE Electron Device Lett.*, vol. 41, no. 7, pp. 997–1000, Jul. 2020.



Zu-Yong Yan was born in Dingxi, Gansu, China. He received the B.E. degree from Shenyang Ligong University, Shenyang, China, and the M.E. degree in physical electronics from the Lanzhou University of Technology, Lanzhou, China. He is currently working toward the Ph.D. degree in electronic science and technology supervised by Prof. Weihua Tang with the Beijing University of Posts and Telecommunications, Beijing, China. His current research focuses on Gallium Oxide photodetectors.



Shan Li was born in Yunmeng, Hubei, China. He received the B.E. and M.E. degrees in materials science and engineering from Xiangtan University, Xiangtan, China, in 2012 and 2015, respectively. He is currently working toward the Ph.D. degree in electronic science and technology supervised by Prof. Weihua Tang with the Beijing University of Posts and Telecommunications, Beijing, China. His research focuses on construction of self-powered Ga_2O_3 -based solar-blind detector.



Zeng Liu was born in Shenyang, Liaoning, China. He received the B.S. degree in physics from Liaoning Normal University, Dalian, China, in 2013, the M.S. degree in plasma physics from the Dalian University of Technology, Dalian, China, in 2016, and the Ph.D. degree in electronic science and technology from the Beijing University of Posts and Telecommunications, Beijing, China, in 2021. Since 2021, he has been an Associate Professor with the College of Electronic and Optical Engineering & College of Microelectronics, Nanjing University of Posts and Telecommunications, Nanjing, China. His current research interests include wide bandgap semiconductors photodetectors and power electronics.



Xiao-Hang Li received the B.S. and M.S. degrees from the Huazhong University of Science and Technology, Wuhan, China, and Lehigh University, Bethlehem, PA, USA, and the Ph.D. degree from The Georgia Institute of Technology, GA, USA, in 2015. He is currently an Associate Professor with King Abdullah University of Science and Technology, Thuwal, Saudi Arabia



Wen-Jie Liu received the bachelor's degree from the School of Energy and Power Engineering, Jiangsu University, Zhenjiang, China, in 2019. Since 2020, under the guidance of Professor Qiao Fen, he has been began to study for the Postgraduate degree with the School of Energy and Power Engineering, Jiangsu University. His current research focuses on supercapacitor electrode materials based on transition metals.



development.

Jian-Ying Yue was born in Datong, Shanxi Province. She received the bachelor's degree from Shanxi Datong University, Datong, China, in 2014 and the master's degree from the Beijing University of Technology, Beijing, China, in 2017. Since 2020, under the guidance of Professor Tang Weihua, she has been studied for the Doctorate degree in electronic science and technology with the Beijing University of Posts and telecommunications, Beijing, China. Her current main research interests include wide band gap semiconductor material growth, research, and



Fen Qiao received the Ph.D. degree from the Dalian University of Technology, Dalian, China, in 2010. She is currently a Professor with Jiangsu University, Zhenjiang, China. Her current research interests include functional micro/nano materials and optoelectronic devices.



Yu-Feng Guo (Member, IEEE) received the bachelor's and master's degrees from Sichuan University, Chengdu, China, in 1996 and 2001, respectively, and the Ph.D. degree from the University of Electronic Science and Technology of China, Chengdu, China, in 2015. He is currently a Full Professor with the Nanjing University of Posts and Telecommunications, Nanjing, China. During 2005–2007, he was a Postdoctoral Research Fellow with Southeast University, Nanjing, China. He is a Senior Member of the *Chinese Institute of Electronics*.



and Italian Institute of Technology, Italy, from 2009 to 2010. From 2016 to 2018, he was a Visiting Scholar with Tulane University, New Orleans, LA, USA. His current research interests include Gallium Oxide electronics and optoelectronics.

Pei-Gang Li received the bachelor's degree from Lanzhou Jiaotong University, Lanzhou, China, the master's degree from Northeast University, Shenyang, China, and the Ph.D. degree from the Institute of Physics, Chinese Academy of Sciences, Beijing, China. He is currently a Full Professor with the Beijing University of Posts and Telecommunications, Beijing, China. He was a Humboldt Scholar with Forschungszentrum Jülich, Germany, from 2007 to 2009, and a Marie Curie Scholar with the Greek Institute of Electronic Structures and Lasers, Greek,



ing Scholar with the National Research Center, France, The University of Hong Kong, Hong Kong, National Institute of Standards and Technology, and Tulane University, New Orleans, LA, USA. He was selected in Hundred-Talent Program of CAS (2001), National candidate of New Century Talent Project (2006) and enjoyed special government allowance (2014). His current research interests mainly include Gallium Oxide photodetectors and power devices fabrications and characterizations.

Wei-Hua Tang received the B.S. and M.S. degrees from Nanjing Normal University, Nanjing, China, and Beijing Normal University, Beijing, China, and the Ph.D. degree from the Institute of Physics, Chinese Academy of Sciences, Beijing, China. He is currently a Full Professor with the Nanjing University of Posts and Telecommunications, Nanjing, China. From 1994 to 2005, he was a Professor with the Institute of Physics, Chinese Academy of Sciences. From 2006 to 2011, he was a Full Professor with Zhejiang Sci-Tech University, Hangzhou, China. He was a Senior Visiting Scholar with the National Research Center, France, The University of Hong Kong, Hong Kong, National Institute of Standards and Technology, and Tulane University, New Orleans, LA, USA. He was selected in Hundred-Talent Program of CAS (2001), National candidate of New Century Talent Project (2006) and enjoyed special government allowance (2014). His current research interests mainly include Gallium Oxide photodetectors and power devices fabrications and characterizations.



Xiao Tang received the B.S. and M.S. degrees from the Hunan University, Changsha, China, and Beijing University of Technology, Beijing, China, and the Ph.D. degree from the Technical University of Denmark, Roskilde, Denmark, in 2013. He is currently a Researcher with the King Abdullah University of Science and Technology, Thuwal, Saudi Arabia.